http://dx.doi.org/10.5935/0103-5053.20140238

J. Braz. Chem. Soc., Vol. 25, No. 12, 2304-2313, 2014.
Printed in Brazil - ©2014 Sociedade Brasileira de Química
0103 - 5053 $6.00+0.00

Article

Cadmium and Tin Magnetic Nanocatalysts Useful for Biodiesel Production

Melquizedeque B. Alves, Fernando C. M. Medeiros, Marcelo H. Sousa, Joel C. Rubim and Paulo A. Z. Suarez*

Laboratório de Materiais e Combustíveis, Instituto de Química, Universidade de Brasília, C.P. 04478, 70904-970 Brasília-DF, Brazil

Nanopartículas magnéticas compostas por óxidos mistos de ferro/cádmio (ICdO) e ferro/estanho (ISnO) foram usadas como catalisadores em reações relevantes para diferentes tecnologias de produção de biodiesel. Estes compostos foram ativos para hidrólise e transesterificação de óleo de soja, bem como para a esterificação de ácidos graxos obtidos a partir do óleo de soja. Na esterificação mediada por ISnO foram alcançados altos rendimentos, ca. 84%, após 1 h de reação a 200 ºC. O óxido foi recuperado magneticamente e reutilizado quatro vezes sem perda da sua atividade catalítica, enquanto que uma perda significativa foi observada quando ICdO foi usado. ISnO demonstrou também atividade para a produção de biodiesel a partir de óleo de macaúba, um substrato altamente ácido.

Magnetic mixed iron/cadmium (ICdO) and iron/tin (ISnO) oxide nanoparticles were used as catalysts in relevant reactions for biodiesel production technologies. These compounds were active for hydrolysis and transesterification of soybean oil as well as esterification of soybean oil fatty acids. In the esterification assisted by ISnO high yields, ca. 84%, were achieved, after 1 h reaction at 200 ºC. The oxide was magnetically recovered and reused four times without loss in its activity, while a loss of activity was observed for ICdO catalyst. ISnO also demonstrated catalytic activity for macauba oil, a highly acidic substrate.

Keywords: ferrites, biodiesel, hydrolysis, esterification, transesterification

Introduction

In order to address the increasing demand for energy and growing ecological awareness, biofuels have emerged in the last decades as elegant alternatives to fossil fuels, since they are obtained from renewable sources.[1] In this sense, biodiesel has been highlighted due to the versatility of raw materials that can be used. Moreover, global population and living standards have risen considerably in recent years and one expects that in the coming decades the demand for food may strongly increase. Thus, the search for raw materials for an environmentally friendly fuel supply must consider its impact in the production of food. Therefore, improvements in the technology to produce renewable fuels are needed to gracefully meet global demand for both food and biofuels, avoiding the food, energy, and environment trilemma.[2]

Regarding the search for raw materials for biodiesel production that avoids the competition with food supply, it is possible to obtain large amounts of fatty materials from different sources: (*i*) acid stocks produced during physical neutralization of fats and oils; (*ii*) domestic or industrial sludge; poultry, porcine or cattle slaughterhouse wastes; (*iii*) algae bioreactors; (*iv*) fish oil; or (*v*) non-edible palm tree oils. However, their main drawback is their high free fatty acid (FA) content, which compromises their use as feedstock in the traditional technology for biodiesel production.[3] One example is a palm tree oil called macauba (*Acrocomia sclerocarpa* M.), which is native to the Brazilian savannah. It is recognized that this palm tree can produce more than 4,000 L *per* ha when associated with cattle.[4] This means that a large amount of oil can be produced in the same area where cattle are reared. Nevertheless, as far as the high FA content of this palm tree oil is concerned (we have received a sample containing about 66% of free fatty acids in its composition), it is impossible to process it using traditional transesterification technologies.

Since 1937, when the first patent regarding biodiesel production was reported,[5] the widespread industrial

*e-mail: psuarez@unb.br

technology is alkaline transesterification, which is not suitable for raw materials containing more than 0.5% free FA in mass due to several issues, like soap formation, which leads to stable emulsions and difficulties to purify biodiesel, and catalyst consumption.[3] In order to address issues of using raw materials with high FA content, different approaches have been described in the literature:

(*i*) Promotes the esterification of free FA using active Brönsted acid catalysts, and then performs the alcoholysis of triacylglycerol (TAG) using transesterification-active alkaline catalysts.[3] More recently, a process to produce biodiesel was developed using the acid stock from the physical neutralization of palm tree oil as raw material, containing 80% of free FA and 20% of TAG.[3] In this technology, after a high conversion rate of FA is achieved using sulfuric acid as catalyst, the biodiesel is recovered by flash distillation and a mixture of unreacted TAG and free FA remains as by-product. Supercritical methanol[6] or catalysts have been used for both esterification and transesterification in combined one-pot[7-10] or two-step biodiesel production.[11-14]

(*ii*) Promotes the complete hydrolysis of TAG in order to convert the raw material into a mixture of fatty acids, and then performs their esterification. Traditionally, the hydrolysis of TAG is carried out within 100-260 ºC and 1-70 bar using 0.4-1.5% m/m initial water-to-oil ratio with or without catalysts.[15] The widespread procedures in the industry are the discontinuous autoclaving, the Twitchell and the continuous countercurrent (Colgate-Emery) processes.[16] New ways to improve the hydrolysis processes have been well studied, some of which involve the use of enzymes,[17-19] Lewis acids catalysts,[20] sub or supercritical systems[21-23] and application of ultrasound.[24,25]

During the last years, we and other researchers have developed solid catalysts with metal Lewis acidity that are active for the production of biodiesel both in batch and in continuous systems.[26,27] The catalysts based on cadmium and tin oxides, particularly pure or mixed with other metals, show excellent results for the reactions of hydrolysis, esterification and transesterification.[13,28-31]

In recent years, magnetic compounds have gained prominence in catalysis. Several studies have metal oxide catalyst precursors that also have magnetic properties. They have applications in many processes with high demands in the petrochemical, pharmaceutical and food industries. Some of the major systems studied involve the use of magnetic materials as supports for catalysts and their application in hydrogenation,[32-37] epoxidation,[38] cross coupling (Suzuki,[39-41] Heck[42] and Sonogashira[43]), oxidation,[44,45] and photodegradation[46,47] reactions. There are also reports of magnetic nanocomposites used to carry enzymes.[48,49] Despite being used as magnetic support, magnetic nanoparticles themselves have shown catalytic activity to reactions like oxidation[50,51] and alkylation.[52,53] Nanostructured magnetic materials have stood out because they allow magnetic separation of the catalysts from the reaction medium. Moreover, they have high surface area that generally increases the catalytic efficiency.[42,50,54] It should be noted that the performance of catalysts is sensitive to particle size, because the surface and electronic properties can vary widely in the nanoscale limits.[55,56]

The aim of this work was to identify new catalytic precursors with potential application in the preparation of biodiesel both using oils with high purity, as well as using a raw material with high free FA contents. In this sense, iron/cadmium and iron/tin magnetic materials were synthesized, which were tested as catalysts in the reactions of hydrolysis, esterification and transesterification of soybean oil and soybean FA. The catalytic activity of the iron/tin catalyst was further investigated in the transesterification/esterification reaction of the crude acid oil from the macauba palm tree.

Experimental

General

All reagents used to prepare the catalysts were obtained from commercial sources and were used without further purification. Refined soybean oil was obtained from commercial sources (Soya) and used as received. Macauba oil was obtained by a traditional procedure that involves fruit pulp pressing. Distilled water was used in the hydrolysis experiments and methanol (Cromoline, 99.8%) was used in the esterification and transesterification assays after drying with magnesium sulfate.

Catalyst synthesis

The catalysts were prepared by an adapted coprecipitation method described in the literature using aqueous solutions of $CdCl_2$ or $SnCl_2$ and $FeCl_3$ in alkaline medium.[57] A solution containing a metal ratio of 2:1 v/v of $FeCl_3$ (0.5 mol L^{-1}) and $CdCl_2$ or $SnCl_2$ (0.5 mol L^{-1}) was quickly added to a 1 L aqueous solution of NaOH (2 mol L^{-1}) at 100 ºC, under vigorous stirring and kept at this condition for 2 h. The obtained dark precipitate was washed with distilled water to remove excess of ions, treated with HNO_3 (1 mol L^{-1}), washed with distilled water and dried in an oven at 100 ºC. The solids were then thermally activated at 300 ºC for 4 h.

Catalyst characterization

The specific surface areas, diameter and pore volume of the catalysts were determined from nitrogen adsorption experiments in a Quantachrome NOVA 2200 analyzer. Before the measurements, the samples were pre-heated at 300 ºC under reduced pressure. The surface acidity analyses were evaluated by temperature-programmed desorption of ammonia (TPD-NH_3) in a Quantachrome ChemBET 3000 instrument equipped with a thermal conductivity detector. The sample was heated up to 400 ºC under continuous flow of helium (80 cm^3 min^{-1}), the ammonia was adsorbed at 100 ºC and the TPD signal was recorded using a temperature ramp of 15 ºC min^{-1}. Powder X-ray diffraction (XRD) measurements were performed on a Bruker D8-Focus Discover diffractometer using radiation of 1.540562 Å (40 kV and 30 mA). Inductively coupled plasma atomic emission spectroscopy (ICP-AES) was used to determine cadmium (228.80 nm), tin (189.99 nm) and iron (259.95 nm) contents in the solids used as catalyst precursors. The samples were previously digested in aqua regia by heating and further analyzed using an ICP Spectroflame model FVM03 with a focal distance of 75 cm, and a concentric Meihard nebulizer (pressure, 38 psi; flux of cooling gas, 13 L min^{-1}; flux of auxiliary gas, 0.5 L min^{-1}; sample injector flow, 1 mL min^{-1}, and forward power of 1.1 kW). The Raman spectra were recorded on a Renishaw InVia Raman system. The spectra were excited at 632.8 nm (HeNe laser) with the laser spot focused on the sample with a 50× objective. The laser power was adjusted in order to avoid sample decomposition.

Catalytic experiments

The catalytic experiments were conducted in a 100 mL stainless steel Parr 5500 Series Compact Reactor using the Parr 4843 controller to control temperature, pressure and mechanical agitation. The reactions were conducted under constant mechanic agitation (800 rpm) and temperature (200 ºC). Due to the vapor pressure of the system, the temperature was measured at the equilibrium pressures. For each reaction (transesterification, esterification or hydrolysis) all reagents were simultaneously added to the reactor, but not mixed until the desired reaction temperature was reached in the reaction bulk. In recycling experiments, the catalyst was separated from the reaction system by using a permanent magnet. The system was kept under a strong magnetic field provided by a neodymium magnet for 15 min in order to ensure maximum recovery of the catalyst. When macauba oil was used, similar procedures were performed.

Reaction analysis

The products of the hydrolysis and transesterification reactions were analyzed by high-performance liquid chromatography (HPLC) in a Shimadzu CTO-20A chromatograph (UV-Vis detection at λ = 205 nm) equipped with a Shim-Pack VP-ODS column (C-18, 250 mm, 4.6 mm i.d.). An injection volume of 20 µL and a flow rate of 1 mL min^{-1} were used in all experiments. The column temperature was held constant at 40 ºC. All samples were dissolved in 2-propanol/hexane (5:4, v/v). An 18.5 min binary gradient with one linear gradient step was employed: 100% methanol in 0 min, 50% methanol and 50% 2-propanol/hexane (5:4, v/v) in 10 min, followed by isocratic elution with the same composition for the last 8.5 min.[58] All solvents were filtered with a 0.45 µm Millipore filter prior to use.

The esterification reaction was analyzed by titration according to standard AOCS Cd3d63 method. The reaction yield *Y(%)* was determined by the relationship between the acidity value of the products (A_p) and reagents (A_r), according to equation 1.

$$Y(\%) = \left(1 - \frac{A_p}{A_r}\right) \times 100 \quad (1)$$

The metal (iron, tin and cadmium) content on some products was also analyzed by ICP-AES in order to evaluate the catalyst leaching degree in the reaction systems studied. The sample opening procedure consisted of weighing 1 g of organic phase followed by the consecutive addition of 1 mL HNO_3, H_2SO_4 and H_2O_2 at 100 ºC. In order to obtain homogeneous aqueous solutions new quantities of these reagents were added after the gas evolution ceased.

Results and Discussion

The details about the mechanism of ferrite formation are still not well understood. It is well accepted that the dissolution of metal salts in water leads to an aqueous complex, which hydrolyzes to form a polymerized aqueous hydroxy complex.[57] It is also known that when two aqueous metal solutions (M^{2+} and Fe^{3+}) are mixed with a hot sodium hydroxide aqueous solution a condensation process takes place, forming a precipitate of a bimetallic oxide (usually ferrites, MFe_2O_4). However, all these possible steps depend on the reaction parameters and may lead to different materials.

Figure 1 shows the diffractograms for iron/cadmium (ICdO) and iron/tin (ISnO) oxides after the coprecipitation reaction and thermal treatment procedures. As observed, a typical system of lines characteristic of the spinel structure

was identified for both obtained precipitates, having a lattice constant nearly equal to that of bulk Fe_3O_4 (see Table 1). It is worth mentioning that no relevant evidence for discrete tin or cadmium oxide phases was observed here. This implies that tin and cadmium have entered the spinel structure by substitution of Fe ions, generating doped $CdFe_2O_4$ and $SnFe_2O_4$ ferrites. Chemical analysis corroborates this fact. Indeed, ICP-AES analysis of the powders at the end of the preparation procedure indicated iron/divalent metal molar ratios of $[Fe^{3+}/Cd^{2+}] = 3.7$ and $[Fe^{3+}/Sn^{2+}] = 3.3$ for ICdO and ISnO materials, respectively.

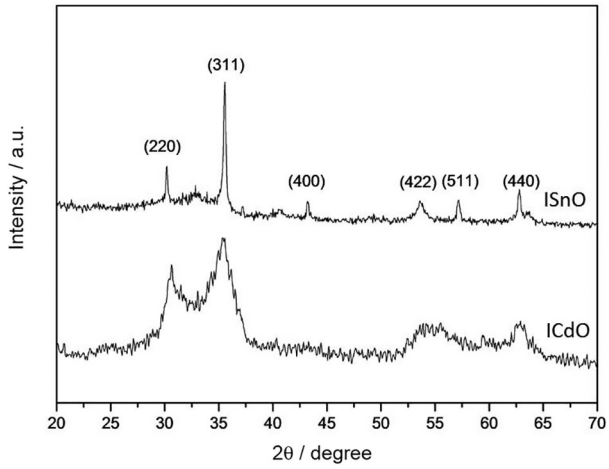

Figure 1. XRD analysis of iron/cadmium (ICdO) and iron/tin (ISnO) oxides.

Additionally, through the Scherrer formula, the broadening of the 311 main peak allowed calculation of the mean crystalline sizes of the grains as 3.5 and 34.8 nm for ICdO and ISnO samples, respectively. Note that these results may be not precise because of the relatively low resolution of the spectra, especially for ICdO.

The magnetic properties of the samples were evaluated by recording the magnetic field (H) dependence on the magnetization (M) at 27 ºC. Thus, the hysteresis loops for the ICdO and ISnO samples are displayed in Figure 2, where magnetizations are normalized by using the sample weight. The ISnO sample presents a loop that shows a ferromagnetic-like behavior with saturation magnetization (M_s), remnant magnetization (M_r) and coercivity (H_c) values of ca. 12.8 emu g^{-1} (at H = 13 kOe), 3.1 emu g^{-1} and 86 Oe, respectively, as shown in the inset of the figure. The M_r/M_s value of 0.24 for ISnO nanoparticles follows the same tendency of the M_r/M_s ratios of 0.09, 0.11 and 0.13 for doped tin ferrites of 4, 10 and 15 nm found in a previous work.[59]

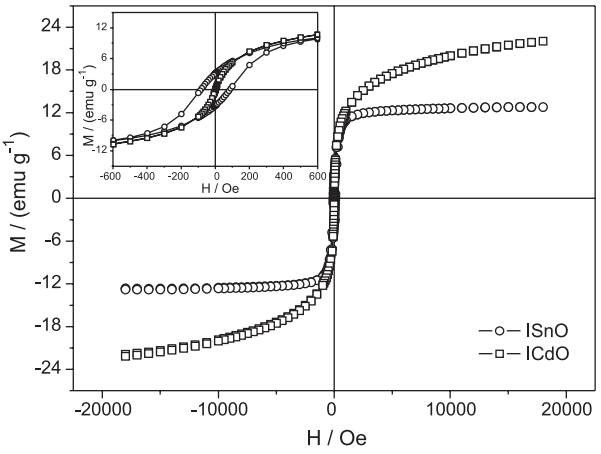

Figure 2. Magnetization curves of the iron/cadmium (ICdO) and iron/tin (ISnO) oxides at 27 ºC.

On the other hand, the ICdO powder displays features of superparamagnetism, with negligible remanence and coercivity in the low field regime.[60] Moreover, the data indicate that ICdO does not saturate in the magnetic field interval investigated in this work, but reaches a magnetization of 22 kOe at the maximum value of magnetic field. This can be explained considering the low dimension

Table 1. Data on catalysts before and after the recycling reactions

		Before reaction	After reaction		
			Transesterification	Esterification	Hydrolysis
ICdO	Catalyst recovered[a] / %	–	79	71	74
	Molar (Fe/Cd) ratio[b]	3.7	10.1	50.3	67.0
	d_{XR}[c] / nm	3.5	7.9	13.7	20.9
	a / Å	8.37	8,41	8.39	8.40
ISnO	Catalyst recovered[a] / %	–	87	90	89
	Molar (Fe/Sn) ratio[b]	3.3	3.4	3.3	3.4
	d_{XR}[c] / nm	34.8	36.2	34.7	33.3
	a / Å	8.38	8.45	8.44	8.42

[a]Percentage (m/m) of catalyst recovered after the fourth recycle; [b]determined by ICP-AES; [c]note that these results may be not precise because of the relatively low resolution of the spectra.

of cadmium-doped ferrite (ca. 3.5 nm) and thus, the well-known finite size and surface magnetization dependence effects.[61,62]

The N_2 sorption isotherms for ICdO and ISnO solids are presented in Figure 3a and Table 2 shows their respective surface areas, pore radius and volumes. As can be depicted from Figure 3, both isotherms present hysteresis by pore condensations that indicate the presence of mesopores (pore diameters between 2 and 50 nm). However, the quantity of nitrogen adsorbed at the low partial pressures (p/p_0) indicates the presence of micropores (pore diameters < 2 nm) in ICdO, which may be responsible for the high surface area of this solid (see Table 2).[63] Moreover, the total pore volume calculated for ICdO is twice the value calculated for ISnO. The isotherm loop profiles also show a morphological feature of these materials; the absence of any limiting adsorption at high p/p_0 is typically attributed to aggregates of plate-like particles giving rise to slit-shaped pores.[63]

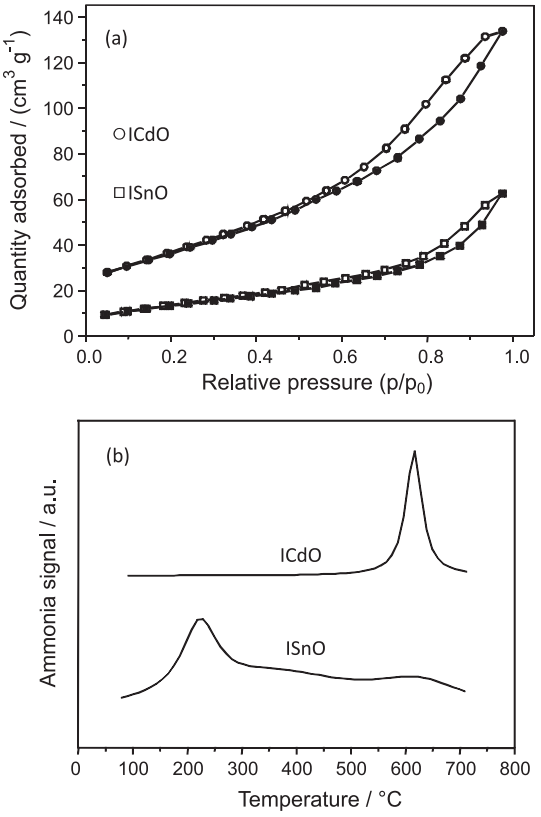

Figure 3. (a) Nitrogen sorption isotherms (the filled markers denote the adsorption branch and the open markers the desorption branch of the isotherm). (b) Temperature-programmed desorption (TPD) of ammonia.

TPD of ammonia, shown in Figure 3b, characterized the strength and distribution of acidic sites: weak near 200 °C, medium near 400 °C and strong near 600 °C.[64] It is accepted that desorption near 600 °C refers only to the Lewis acid sites in these materials, i.e., the acidity in the weak plus medium regions is due to the Brönsted and weaker Lewis acid sites. Thus, in ICdO there are only Lewis acid sites, while in ISnO there are also desorption regions of weak and medium acidity that can be Lewis or Brönsted acid sites.[64] It was reported that in ferrospinels the acidity comes from the metal in M–O bonds, and the electron donor properties of the solids come from the surface hydroxyl, oxygen anions or electron trapped in intrinsic defects.[65]

Table 2. Nitrogen physisorption data of iron/cadmium (ICdO) and iron/tin (ISnO) oxides

	Surface area[a] / (m^2 g^{-1})	Total pore volume / (cm^3 g^{-1})	Average pore radius / nm
ICdO	130.2	0.206	3.169
ISnO	49.9	0.0968	3.883

[a]Multipoint Brunauer-Emmett-Teller (BET).

Catalytic experiments

The catalytic activity of ICdO and ISnO was investigated by transesterification and hydrolysis of triacylglycerides, as well as by the esterification of fatty acids, which are useful reactions for biodiesel production.[29,66] In this sense, the experiments were carried out using soybean oil and fatty acids (previously prepared from soybean oil) as substrate. The reaction yields for esterification, hydrolysis and transesterification are shown in Figure 4. The catalysts are apparently more active for esterification than for transesterification and hydrolysis. It is important to highlight that there is a small contribution by self-catalysis promoted by fatty acids that act as Brönsted catalysts.[14,29,66] To evaluate the self-catalytic behavior of fatty acids we performed an esterification reaction at 200 ºC for 2 h in the absence of catalyst that resulted in 41% yield. Thus, these results suggest that the main catalytic activity is due to the magnetic materials. Indeed, the increasing activity during hydrolysis observed for ICdO and ISnO may also be understood as a result of the catalytic activity of the formed fatty acids.

Recycling experiments

In order to evaluate the efficacy of recovery and reuse of the solids after hydrolysis, esterification or transesterification, the catalyst powders were recovered after reactions using a magnet and the solids were used five times in each type of reaction. After separation, the solid was reintroduced in the reactor without any further treatment and a new charge of substrates was added. In

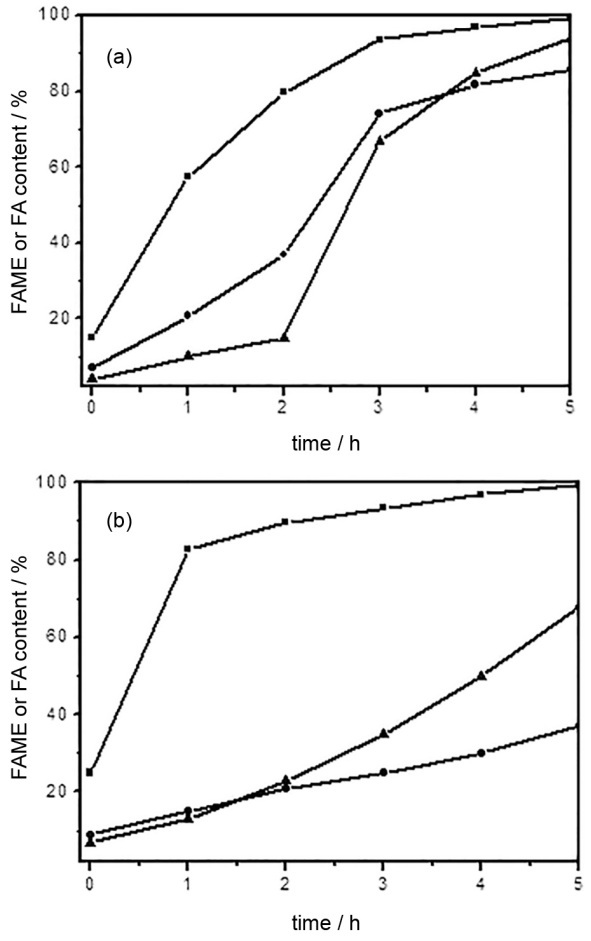

Figure 4. Reactions of transesterification (●), esterification (■) and hydrolysis (▲) using (a) ICdO or (b) ISnO. Conditions: 20 g soybean oil or soybean fatty acid, 6 g methanol or 20 g water and 1 g of ICdO or ISnO, at 200 ºC, 13.6 bar in hydrolysis and 18.6 bar in others.

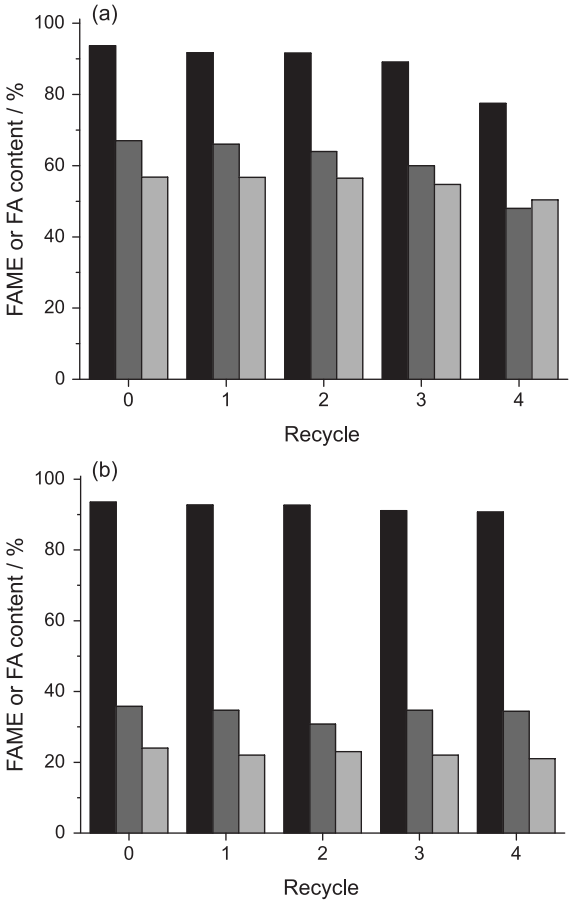

Figure 5. Reactions of esterification (black), hydrolysis (gray) and transesterification (light gray) in recycling experiments with (a) ICdO or (b) ISnO. Conditions: 20 g soybean oil or soybean fatty acid, 6 g methanol or 20 g water, 1 g of ICdO or ISnO, 3 h, at 200 ºC, 13.6 bar in hydrolysis and 18.6 bar in others.

this way, Figure 5 shows there were negligible losses in the catalytic activity of ISnO and a light deactivation of ICdO after the forth recycle.

However, the catalysts showed catalytic activity in five consecutive reactions and it can be stated that in all experiments there was a small loss in the amounts of catalyst initially introduced in the first reaction (see Table 1). Despite the high activity of catalyst ICdO, there is a decrease of its activity after the recycling experiments that may be related to the decrease in the amount of cadmium in the solid composition after the recycles. This can be observed in Table 1, which brings the Fe^{3+}/M^{2+} molar ratio (M = Cd^{2+} for ICdO and Sn^{2+} for ISnO catalysts, respectively), before and after the recycles, as determined by ICP-AES analysis. However, a decrease in ISnO catalyst activity was not observed during recycling experiments; in this case the Fe^{3+}/Sn^{2+} molar ration remained nearly constant along all recycling experiments (see Table 1).

The changes in the catalyst compositions, that were followed by the ICP-AES analysis of the reaction products in the recycle experiments, confirmed there was significant cadmium leaching from ICdO and, in contrast, negligible leaching of tin from the ISnO sample (Table 3). Moreover, the loss of Cd^{2+} is prominent after the first recycling and becomes less significant after the next ones, a fact that should probably be due to chemical (acidity) and physical (temperature and pressure) conditions imposed during the recycles. Thus, owing to the reduced size (i.e., a larger surface area) of ICdO nanograins the loss of cadmium is more accentuated than that of tin in the ISnO sample.

The changes in the chemical composition of the ICdO catalyst during the recycling procedures also modify the crystalline and size characteristics of the nanoparticles as observed in the diffractograms in Figure 6. As mentioned before, the tin-doped ferrite sample does not significantly change its chemical composition (i.e., tin remains in the solid structure) and only about 10% of the solid is lost after the recycles. In this case, the diffractograms after catalysis experiments show a slight improvement on the crystallinity of ISnO nanograins (see Figure 6b), however,

Table 3. Metal content (ppm of Cd or Sn) on the reaction products of the recycle experiments illustrated in Figure 3

Solids used as catalytic precursor	Recycle No.	Transesterification		Esterification		Hydrolysis	
		M^{2+} / ppm	Iron / ppm	M^{2+} / ppm	Iron / ppm	M^{2+} / ppm	Iron / ppm
ICdO	0	4831[a]	893	4570[a]	276	4580[a]	354
	1	354[a]	90	829[a]	43	402[a]	129
	2	139[a]	57	259[a]	14	67[a]	110
	3	79[a]	21	135[a]	24	46[a]	72
	4	60[a]	5	85[a]	6	54[a]	10
ISnO	0	15[b]	4	20[b]	7	16[b]	6
	1	5[b]	3	7[b]	6	5[b]	5
	2	4[b]	1	3[b]	0[c]	0[b,c]	0[c]
	3	3[b]	0[c]	2[b]	0[c]	0[b,c]	0[c]
	4	0[b,c]	0[c]	0[b,c]	0[c]	0[b,c]	0[c]

[a]ppm of cadmium, determined by ICP-AES; [b]ppm of tin, determined by ICP-AES; [c]below the limit of quantification (LOQ). LOQ_{Cd} = 0.00972 ppm; LOQ_{Sn} = 1.53 ppm; LOQ_{Fe} = 0.0277 ppm.

no considerable changes were observed in particle sizes and lattice parameters, as shown in Table 1. On the other hand, the significant loss of cadmium associated with the recycling processes led to prominent alterations on the diffraction patterns of ICdO nanograins, as shown in Figure 6a. Here, the crystallinity of products was improved and particle size increased from 3.5 nm before reaction to values of ca. 7.9, 13.7 and 20.9 nm after the fourth cycle of transesterification, esterification and hydrolysis, respectively. This should probably be due to dissolution of material on the surface of the ICdO nanoparticles and reprecipitation of iron on the remaining ferrite cores. In this way, the spinel structure was preserved and the crystalline size of the nanograins increased.

The Raman spectra of the ICdO and ISnO samples acquired before and after the transesterification, hydrolysis and esterification reactions are displayed in Figure 7. The Raman spectrum of the ICdO sample before reaction (Figure 7a) shows Raman features at 172, 223, 370, 400, 510, 620, and 683 cm^{-1}. Ferrites with spinel structure have cubic symmetry and therefore should only have five Raman active modes.[67] As observed for $CoFe_3O_4$ nanoparticles, the Raman spectrum of the as prepared $CdFe_2O_4$ presents a total of seven Raman features, suggesting that quantum size effects are playing a role causing the breakdown on the momentum conservation rule, as observed before for Fe_3O_4 and $CoFe_2O_4$ nanoparticles.[68] It is worth mentioning that as the ICdO samples are used as the catalyst in three different reactions two main Raman features emerge, one near 300 cm^{-1} and another near 662 cm^{-1}. These features are characteristic of magnetite, as already reported in the literature.[67] These results, in conjunction with those obtained by ICP-AES analysis of the metal content in the reaction products (Table 3), are strong evidences for the formation of a mixed compound during the synthesis of the ICdO catalyst. The mixed compound certainly contains magnetite, as evidenced by the characteristic Raman peaks near 300 and 662 cm^{-1} that emerge after the ICdO sample is exposed to the different reactions.

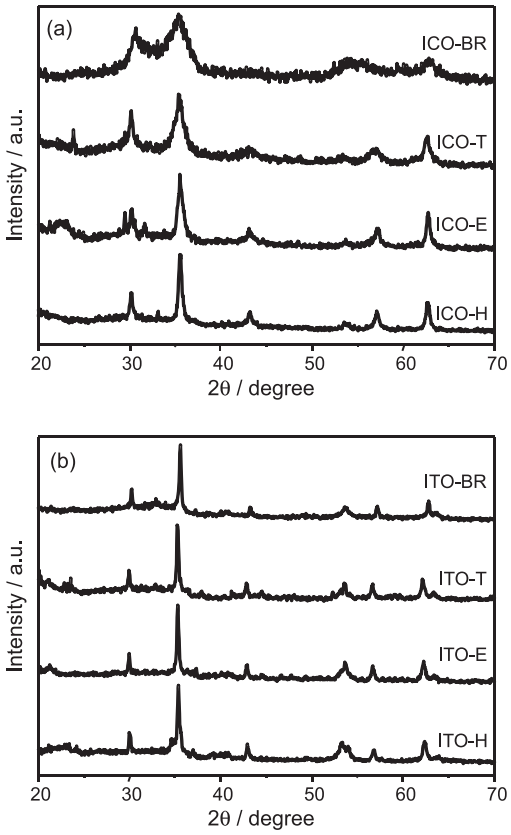

Figure 6. XRD of catalysts (a) ICdO (ICO) and (b) ISnO (ITO) before reaction (BR), after transesterification (T), esterification (E) and hydrolysis (H).

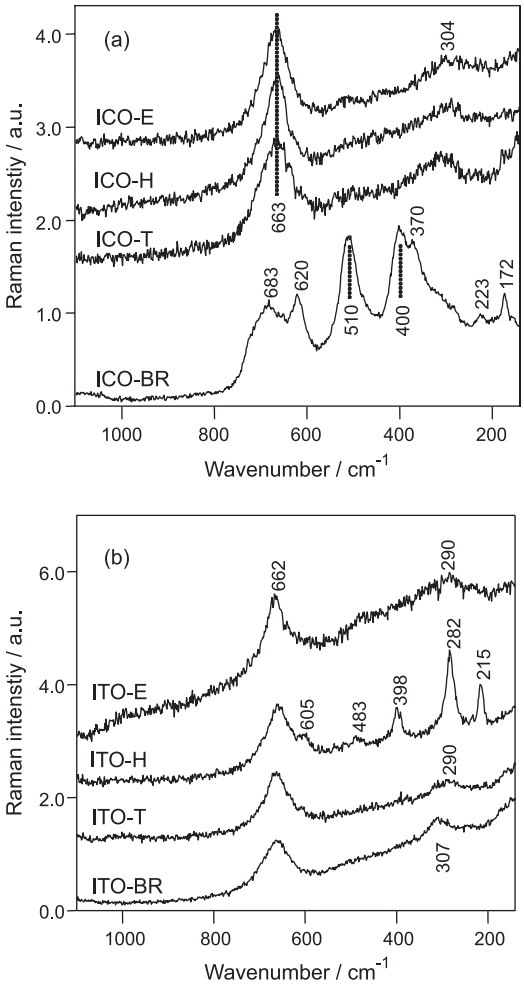

Figure 7. Raman spectra of (a) ICdO (ICO) and (b) ISnO (ITO) samples. BR, T, H, and E stand for samples before and after transesterification, hydrolysis, and esterification reactions, respectively.

The Raman spectra of the ISnO samples before and after the reactions are presented in Figure 7b. In this case, the major features observed are those characteristic of magnetite, near 300 and 662 cm^{-1}. This is an interesting finding, since the replacement of Fe(II) centers by Sn(II) in the spinel structure of ferrite does not cause a significant change in the Raman phonons. However, for the samples used in the hydrolysis reaction, other Raman features are observed at 215, 282, 398, 483, and 605 cm^{-1} which are characteristic of the α-Fe_2O_3 phase. One could argue that the formation of the α-Fe_2O_3[69] phase is due to the laser heating. However, these features were not observed in the other Raman spectra presented in Figure 7b. As mentioned in the experimental section, the laser power was adjusted to a lower level, just to avoid sample oxidation. Because there is no evidence by XRD analysis of the formation of hematite during the hydrolysis reaction, these Raman signals possibly refer to a short phase of α-Fe_2O_3 in the sample where the laser was focused.

Fatty acid methyl ester (FAME) production using macauba oil assisted by ISnO

For the reasons presented in the Introduction section it is interesting to evaluate the potential of the tin catalyst for the production of biodiesel using a low-grade raw material (high free fatty acid content). In this sense, a study using a sample from the macauba palm tree oil was carried out.

Figure 8 shows the results obtained after the reaction of macauba oil with methanol in the presence of ISnO. Note that only the ISnO catalyst was used because its performance was superior when compared to ICdO in the recycling experiments. It is noteworthy that both esterification and transesterification reactions take place in this experiment, given that the substrate contains, in addition to glycerides, a high content of fatty acids. During the reaction there is a decrease in the acidity value, sharper at the first 2 h, reaching a low acidity, which indicates that free fatty acids were esterified producing biodiesel. On the other hand, up to 90% of fatty acid methyl ester (FAME) was obtained after 3 h of reaction, as a result of acyl-glyceride transesterification and fatty acid esterification. After the reaction, the ISnO catalyst was recovered by

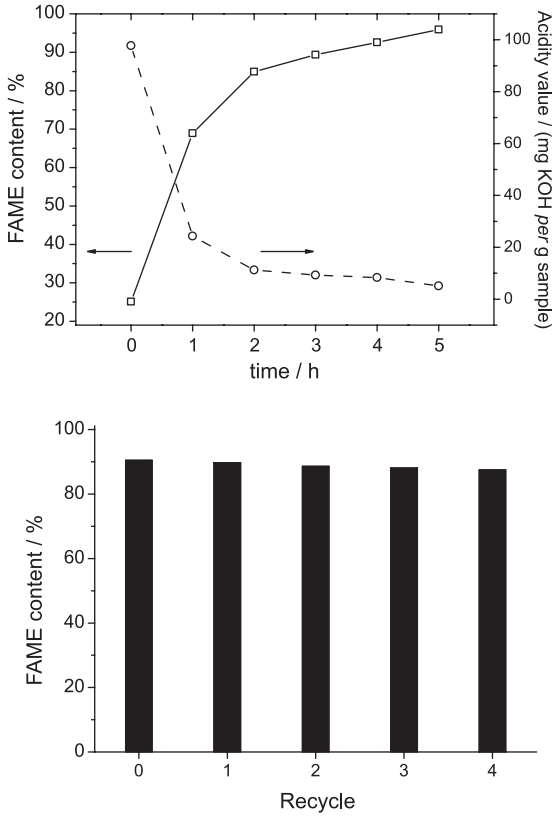

Figure 8. Reactions using macauba oil and methanol in the presence of solid ISnO. (a) Conversion of FAME and acidity value as a function of reaction time; (b) conversion to FAME after 3 h of reaction for five charges of substrates using the same catalyst. Conditions: 20 g oil, 6 g methanol, 1 g catalyst, at 200 ºC, 18.6 bar.

magnetic separation and was reused four other times with new charges of substrate. As can be depicted from Figure 8b, it was possible to recover the catalyst with no significant loss of activity.

Conclusions

Mixed iron/cadmium (ICdO) and iron/tin (ISnO) oxides were prepared and tested as catalysts in biodiesel production through hydrolysis, esterification and transesterification reactions using soybean oil or their fatty acids. The metal oxide catalysts present large surface areas. The surface area of the ICdO catalyst was twice that of ISnO. Despite this difference in surface area no significant catalytic activity difference was observed in the esterification reaction. The highest catalytic activity in the esterification of soybean fatty acids was presented by the ISnO catalyst with a 84% yield in FAME after 1 h reaction at 200 ºC. ICdO catalyst showed higher activities in the hydrolysis and transesterefication reactions, probably due to its larger density of Lewis acid sites. The mixed metal catalysts were shown to be nanostructured materials with spinel structures and presented magnetic behavior, ISnO is ferromagnetic and ICdO is superparamagnetic, which allows their magnetic recovery after the reactions. The ISnO catalyst did not present any significant change in the structure after the reactions and showed excellent potential for reuse. It was reused four times in recycling reactions without loss of catalytic activity. ICdO, on the contrary, presented considerable changes in the structure after the reactions and showed considerable loss of Cd during the recycling experiments. Due to its potential for reuse as a catalyst, ISnO was tested in a transeterification/esterification reaction using macauba oil. Nearly 90% of FAME conversion was obtained after 3 h reaction time and the ISnO catalytic activity remained high even after four recycles. These results strongly suggest that macauba oil can be an excellent alternative to biodiesel production, since the oil can be produced in consortium with cattle.

Acknowledgements

We would like to thank INCT-Catálise, CAPES, CNPq and FAPDF for partial financial support. The authors are in debt with CNPq for their research fellowships. The authors of this work had the opportunity to meet Roberto F. De Souza. Some had the great opportunity to enjoy a major interaction with him. Regardless of the level of interaction each one has had with him, everyone recognizes him as a great human being, teacher and researcher and dedicate this work to his memory.

References

1. Brandão, R. F.; Quirino, R. L.; Mello, V. M.; Tavares, A. P.; Peres, A. C.; Guinhos, F.; Rubim, J. C.; Suarez, P. A. Z.; *J. Braz. Chem. Soc.* **2009**, *20*, 954.
2. Tilman, D.; Socolow, R.; Foley, J. A.; Hill, J.; Larson, E.; Lynd, L.; Pacala, S.; Reilly, J.; Searchinger, T.; Somerville, C.; Williams, R.; *Science* **2009**, *270*, 325.
3. Suarez, P. A. Z.; Santos, A. L. F.; Rodrigues, J. P.; Alves, M. B.; *Quim. Nova* **2009**, *32*, 768.
4. Bhering, L.; *Biodieselbr* **2010**, *Ago/set*, 60.
5. Chavanne, G.; *BE pat. 422,877* **1937** *(CA 1938, 32, 4313).*
6. Kusdiana, D.; Saka, S.; *J. Chem. Eng. Jpn.* **2001**, *34*, 383.
7. Yan, S.; Salley, S. O.; Simon, K. Y.; *Appl. Catal., A* **2009**, *353*, 203.
8. Sreeprasanth, P. S.; Srivastava, R.; Srinivas, D.; *Appl. Catal., A* **2006**, *314*, 148.
9. Li, J.; Wang, X. H.; Zhu, W. M.; Cao, F. H.; *ChemSusChem* **2009**, *2*, 177.
10. Suwannakarn, K.; Lotero, E.; Ngaosuwan, K.; Goodwin Jr., J. G.; *Ind. Eng. Chem. Res.* **2009**, *48*, 2810.
11. Park, Y. M.; Lee, D. W.; Kim, D. K.; Lee, J. S.; Lee, K. Y.; *Catal. Today* **2008**, *131*, 238.
12. Marchetti, J. M.; Miguel, V. U.; Errazu, A. F.; *Fuel* **2007**, *86*, 906.
13. Macêdo, C. C. S.; Abreu, F. R.; Alves, M. B.; Tavares, A. P.; Zara, L. F.; Rubim, J. C.; Suarez, P. A. Z.; *J. Braz. Chem. Soc.* **2006**, *17*, 1291.
14. Mello, V. M.; Pousa, G. P. A. G.; Dias, I. M.; Suarez, P. A. Z.; *Fuel Process. Technol.* **2011**, *92*, 53.
15. Patil, T. A.; Butala, D. N.; Raghunathan, T. S.; Shankar, H. S.; *Ind. Eng. Chem. Res.* **1988**, *27*, 727.
16. Shreve, R. N.; Brink Jr., J. A.; *Chemical Process Industries*, 5th ed.; McGraw-Hill: New York, 1984.
17. Freitas, L.; Bueno, T.; Perez, V. H.; Santos, J. C.; de Castro, H. F.; *World J. Microbiol. Biotechnol.* **2007**, *23*, 1725.
18. Noureddini, H.; Gao, X.; Joshi, S.; *J. Am. Oil Chem. Soc.* **2003**, *80*, 1077.
19. Ting, W. J.; Tung, K. Y.; Giridhar, R.; Wu, W. T.; *J. Mol. Cat. B: Enzym.* **2006**, *42*, 32.
20. Ngaosuwan, K.; Lotero, E.; Suwannakarn, K.; Goodwin Jr., J. G.; Praserthdam, P.; *Ind. Eng. Chem. Res.* **2009**, *48*, 4757.
21. King, J. W.; Holliday, R. L.; List, G. R.; *Green Chem.* **1999**, *1*, 261.
22. Holliday, R. L.; King, J. W.; List, G. R.; *Ind. Eng. Chem. Res.* **1997**, *36*, 932.
23. Moquin, P. H. L.; Temelli, F.; *J. Supercrit. Fluids* **2008**, *45*, 94.
24. Bhatkhande, B. S.; Samant, S. D.; *Ultrason. Sonochem.* **1998**, *5*, 7.
25. Entezari, M. H.; Keshavarzi, A.; *Ultrason. Sonochem.* **2001**, *8*, 213.

26. Suarez, P. A. Z.; Silva, F. M.; *J. Braz. Chem. Soc.* **2012**, *23*, 1201.
27. Silva, F. M.; Pinho, D. M. M.; Houg, G. P.; Reis, I. B. A.; Kawamura, M.; Quemel, M. S. R.; Montes, P. R.; Suarez, P. A. Z.; *Chem. Eng. Res. Des.* **2014**, *92*, 1463.
28. Abreu, F. R.; Alves, M. B.; Macêdo, C. C. S.; Zara, L. F.; Suarez, P. A. Z.; *J. Mol. Catal. A: Chem.* **2005**, *227*, 263.
29. Alves, M. B.; Medeiros, F. C. M.; Suarez, P. A. Z.; *Ind. Eng. Chem. Res.* **2010**, *49*, 7176.
30. Yan, S.; Salley, S. O.; Simon Ng, K. Y.; *Appl. Catal., A* **2009**, *353*, 203.
31. Ngaosuwan, K.; Lotero, E.; Suwannakarn, K.; Goodwin Jr., J. G.; Praserthdam, P.; *Ind. Eng. Chem. Res.* **2009**, *48*, 4757.
32. Baruwati, B.; Polshettiwar, V.; Varma, R. S.; *Tetrahedron Lett.* **2009**, *50*, 1215.
33. Guin, D.; Baruwati, B.; Manorama, S. V.; *Org. Lett.* **2007**, *9*, 1419.
34. Hu, A.; Yee, G. T.; Lin, W.; *J. Am. Chem. Soc.* **2005**, *127*, 12486.
35. Rossi, L. M.; Vono, L. L. R.; Silva, F. P.; Kiyohara, P. K.; Duarte, E. L.; Matos, J. R.; *Appl. Catal., A* **2007**, *330*, 139.
36. Polshettiwar, V.; Baruwati, B.; Varma, R. S.; *Green Chem.* **2009**, *11*, 127.
37. Rossi, L. M.; Silva, F. P.; Vono, L. L. R.; Kiyohara, P. K.; Duarte, E. L.; Itri, R.; Landersc, R.; Machado, G.; *Green Chem.* **2007**, *9*, 379.
38. Shokouhimehr, M.; Piao, Y.; Kim, J.; Jang, Y.; Hyeon, T.; *Angew. Chem., Int. Ed.* **2007**, *46*, 7039.
39. Duanmu, C.; Saha, I.; Zheng, Y.; Goodson, B. M.; Gao, Y.; *Chem. Mater.* **2006**, *18*, 5973.
40. Zheng, Y.; Stevens, P. D.; Gao, Y.; *J. Org. Chem.* **2006**, *71*, 537.
41. Stevens, P. D.; Fan, J.; Gardimalla, H. M. R.; Yen, M.; Gao, Y.; *Org. Lett.* **2005**, *7*, 2085.
42. Baruwati, B.; Guin, D.; Manorama, S. V.; *Org. Lett.* **2007**, *9*, 5377.
43. Liu, J.; Peng, X.; Sun, W.; Zhao, Y.; Xia, C.; *Org. Lett.* **2008**, *10*, 3933.
44. Zhang, X.; Yan, J.; Han, S.; Shioyama, H.; Xu, Q.; *J. Am. Chem. Soc.* **2009**, *131*, 2778.
45. Silva, J. B.; Diniz, C. F.; Lago, R. M.; Mohallem, N. D. S.; *J. Non-Cryst. Solids* **2004**, *348*, 201.
46. Ao, Y.; Xu, J.; Shen, X.; Fu, D.; Yuan, C.; *J. Hazard. Mater.* **2008**, *160*, 295.
47. Ao, Y.; Xu, J.; Fu, D.; Shen, X.; Yuan, C.; *Sep. Purif. Technol.* **2008**, *61*, 436.
48. Gao, X.; Yu, K. M. K.; Tam, K. Y.; Tsang, S. C.; *Chem. Commun.* **2003**, 2998.
49. Yang, H.; Zhang, S.; Chen, X.; Zhuang, Z.; Xu, J.; Wang, X.; *Anal. Chem.* **2004**, *76*, 1316.
50. Guin, D.; Baruwati, B.; Manorama, S. V.; *J. Mol. Catal. A: Chem.* **2005**, *242*, 26.
51. Ramanathan, R.; Sugunan, S.; *Catal. Commun.* **2007**, *8*, 1521.
52. Ghorpade, S. P.; Darshane, V. S.; Dixit, S. G.; *Appl. Catal., A* **1998**, *166*, 135.
53. Sreekumar, K.; Mathew, T.; Devassy, B. M.; Rajgopal, R.; Vetrivel, R.; Rao, B. S.; *Appl. Catal., A* **2001**, *205*, 11.
54. Jacinto, M. J.; Kiyohara, P. K.; Masunaga, S. H.; Jardim, R. F.; Rossi, L. M.; *Appl. Catal., A* **2008**, *338*, 52.
55. Bell, A. T.; *Science* **2003**, *299*, 1688.
56. Van Santen, R. A.; *Acc. Chem. Res.* **2009**, *42*, 57.
57. Sousa, M. H.; Tonrinho, F. A.; Depeyrot, J.; da Silva, G. J.; Lara, M. C. F. L.; *J. Phys. Chem. B* **2001**, *105*, 1168.
58. Carvalho, M. S.; Mendonça, M. A.; Pinho, D. M. M.; Resck, I. S.; Suarez, P. A. Z.; *J. Braz. Chem. Soc.* **2012**, *23*, 763.
59. Liu, F.; Li, T.; Zheng, H.; *Phys. Lett. A* **2004**, *323*, 305.
60. Morais, P. C.; Silva, O.; Gravina, P. P.; Figueiredo, L. C.; Lima, E. C. D.; Silva, L. P.; Azevedo, R. B.; Neto, K. S.; *IEEE Trans. Magn.* **2003**, *39*, 2639.
61. Aquino, R.; Depeyrot, J.; Sousa, M. H.; Tourinho, F. A.; Dubois, E.; Perzynski, R.; *Phys. Rev. B: Condens. Matter Mater. Phys.* **2005**, *72*, 184435.
62. Sousa, E. C.; Sousa, M. H.; Goya, G. F.; Rechenberg, H. R.; Lara, M. C. F. L.; *J. Magn. Magn. Mater.* **2004**, 272.
63. Sing, K. S. W.; Everett, D. H.; Haul, R. A. W.; Mouscou, L.; Pierotti, R. A.; Rouquerol, J.; Siemiemiewska, T.; *Pure Appl. Chem.* **1985**, *57*, 603.
64. Rezende, M. J. C.; Pereira, M. S. C.; Santos, G. F. N.; Aroeira, G. O. P.; Albuquerque Jr., T. C.; Suarez, P. A. Z.; Pinto, A. C.; *J. Braz. Chem. Soc.* **2012**, *23*, 1209.
65. Corddischi, D.; Indovina, V.; *J. Chem. Soc., Faraday Trans. 1* **1976**, *72*, 2341.
66. Brito, Y. C.; Ferreira, D. A. C.; Fragoso, D. M. A.; Mendes, P. R.; de Oliveira, C. M. J.; Meneghetti, M. R.; Meneghetti, S. M. P.; *Appl. Catal., A* **2012**, *443-444*, 202.
67. White, W. B.; Deangelis, B. A.; *Spectrochim. Acta, Part A* **1967**, *23*, 985.
68. Jacintho, G. V. M.; Brolo, A. G.; Corio, P.; Suarez, P. A. Z.; Rubim, J. C.; *J. Phys. Chem. C* **2009**, *113*, 7684.
69. Faria, D. L. A.; Silva, S. V.; Oliveira, M. T.; *J. Raman Spectrosc.* **1997**, *28*, 873.

Submitted: July 20, 2014
Published online: October 10, 2014